Food Hydrocolloids 123 (2022) 107170

Contents lists available at ScienceDirect

Food Hydrocolloids

journal homepage: www.elsevier.com/locate/foodhyd

Gelation and network structure of acidified milk gel investigated at different length scales with and without addition of *iota*-carrageenan

Izumi Sone [a,*], Moe Hosoi [b], Lester C. Geonzon [c], Hwabin Jung [b], Faith Bernadette Descallar [b], Hu Bingjie [d], Shingo Matsukawa [b]

[a] Nofima AS, Muninbakken 9-13, Breivika, 9019, Tromsø, Norway
[b] Department of Food Science and Technology, Tokyo University of Marine Science and Technology, 4-5-7 Konan, Minato-ku, Tokyo, 108-8477, Japan
[c] Department of Life and Environmental Sciences, University of Tsukuba, 1-1-1 Tennoudai, Ibaraki, 305-8572, Tsukuba, Japan
[d] Shandong University of Technology, No.266 West Xincun Road, Zhangdian District, Zibo, 255000, China

ARTICLE INFO

Keywords:
Acid milk gel
Iota-carrageenan
Particle tracking
Pulsed field gradient NMR

ABSTRACT

This work investigated the formation of acid milk gel at different length scales with and without the addition of *iota*-carrageenan (IC) (0.5% w/w) during incubation at 30 °C, using bulk rheology and syringe compression test at the macroscopic level, passive particle tracking (particle diameter 0.3 μm and 1.0 μm) at the microscopic level and pulsed field gradient (PFG)-NMR with poly(ethylene oxide) (PEO) at the molecular level. IC induced the early formation of the gel network in the sample as demonstrated by the progressive G′ and G″ increase (where $G' > G''$) in the macroscopic measurement. When repeatedly compressed at the developing stage, the formed gel network in the IC sample reassociated into non-native colloidal structures unable to contain the serum phase, which also occurred without IC but at later incubation stage. The increased PEO diffusion at 30 min in PFG-NMR reflected the emerging casein-casein network and its extensive rearrangement occurring at the molecular level in both samples. This corresponded with the mean square displacement of the probe particles with IC at 30 min but not without IC, indicating that IC altered the length scale of the network rearrangements occurring at the molecular level to be detected at the microscopic level in the particle tracking. The size-dependent particle behaviors in the particle tracking demonstrated a high degree of IC-induced network heterogeneity that continued to develop even at late incubation stage, on contrary to the drastic compaction of the formed network observed in the sample without IC.

1. Introduction

Acid milk gelation is an essential mechanism in the manufacture of common dairy products such as yoghurt. Milk acidification can be induced using glucono-*δ*-lactone (GDL) where the hydrolysis of GDL to gluconic acid results in a gradual reduction in pH (Lucey, Tamehana, Singh, & Munro, 1998). The formation and physical properties of acidified milk gels have been extensively studied by bulk rheology (Lucey, 2016) where the microscopic properties of the sample such as micro-viscoelasticity are averaged even in complex colloidal systems where spatial heterogeneity can exist within and between a coarse particulate network (Cucheval, Vincent, Hemar, Otter, & Williams, 2009). Microscopic imaging techniques such as confocal laser scanning microscopy (CLSM) (Lucey et al., 1998), scanning electron microscopy (SEM) (Martin, Douglas Goff, Smith, & Dalgleish, 2006; Pang, Deeth, Sharma, & Bansal, 2015) and transmission electron microscopy (TEM) (McMahon, Du, McManus, & Larsen, 2009) provide direct information on the microstructure but entail extensive drying (for SEM), staining (for TEM) or fluorophore labelling (for CSLM), potentially obscuring the actual gel structure and gelation mechanism.

Pulsed field gradient NMR (PFG-NMR) is an emerging powerful tool that enables non-destructive investigation of molecular mobility of polymers in liquid and gel states (Price, 2009). The diffusion coefficient (*D*) of probe polymers, such as poly(ethylene glycol)s (PEGs) and poly (ethylene oxide) (PEOs) reflects the local environment of interspaces in the host network, allowing molecular level investigation of the gelling mechanism and structure of colloidal systems (Hu, Lu, Zhao, & Matsukawa, 2017). Applied to casein suspensions and in gels, use of the PFG-NMR technique has demonstrated size- and concentration-dependent changes in the *D* of PEGs with different

* Corresponding author. Department of Processing Technology, Nofima AS, Stavanger, Norway.
E-mail address: Izumi.Sone@Nofima.no (I. Sone).

https://doi.org/10.1016/j.foodhyd.2021.107170
Received 15 April 2021; Received in revised form 30 July 2021; Accepted 1 September 2021
Available online 4 September 2021

molecular weights (6×10^2 to 5×10^5) upon acidification, signalizing the de(hydration) of casein particles and structural re-organization of the network (Colsenet, Soderman, & Mariette, 2005; Le Feunteun & Mariette, 2008a; Salami, Rondeau-Mouro, van Duynhoven, & Mariette, 2013).

Particle tracking is another non-invasive technique increasingly used to investigate the microscopic viscoelastic properties of complex colloidal systems. In this approach, micron-sized probe particles are dispersed in the medium and the Brownian motion of the individual particles are tracked based on signatures of the corresponding mean square displacement (msd) (Caggioni, Spicer, Blair, Lindberg, & Weitz, 2007; Moschakis, 2013). Moreover, particle tracking enables spatial mapping of the microviscoelastic properties of complex fluids (typically <1 Pa), provided that appropriate size and concentration of probe particles are used (Valentine et al., 2004). Particle tracking method is also complementary to the PFG-NMR technique which requires probe molecules or polymers with a diameter smaller than 0.1 μm (Balakrishnan, Durand, & Nicolai, 2011). Using this technique, Moschakis, Murray, and Dickinson (2010) probed emerging structural heterogeneity in the casein network relating to the non-Gaussian distribution of the MSDs, which reflected different sizes and shapes of casein aggregates in the system upon acidification. Cucheval et al. (2009) observed a similar pattern in the development of the particle MSDs and non-Gaussian distribution regardless of pectin addition (0.2% w/w).

Carrageenan is a sulfated polysaccharide added in dairy products at low dosage to strengthen the casein network towards viscosity and gelation enhancement and reduction of syneresis (Langendorff et al., 1999). In milk, behavioral differences exist between the three carrageenan forms and at different concentrations. *Iota*- (IC) and *kappa*--carrageenan (KC) adsorb to the casein micelles only when in helix form (i.e., at temperatures below 45 °C) in the presence of cations such as K+ and Ca^2 + present in milk (Drohan, Tziboula, McNulty, & Horne, 1997; Ji, Corredig, & Goff, 2008), while *lambda*-carrageenan adsorbs regardless of temperature between 25 and 60 °C (Langendorff et al., 2000). Negatively charged KC and IC helices interact with the positively charged surface of casein micelles (region of *k*-casein), possibly through the involvement of the sulphate groups on the carrageenan (Spagnuolo, Dalgleish, Goff, & Morris, 2005). Their interaction is also affected by environmental factors such as pH, ionic strengths, calcium content, processing methods and addition of other polysaccharides (Acero-Lopez, Alexander, & Corredig, 2010; Cavallieri, Fialho, & Cunha, 2011; Corredig, Sharafbafi, & Kristo, 2011; Ji et al., 2008). Although previous studies have investigated the interaction of milk systems with IC, few have conducted multi-length-scale investigation of acid milk gelation at the macro-, micro- and molecular level to demonstrate the formation of network structure and spatial heterogeneity in milk gel as affected by IC at low concentration.

This work investigated the formation of acid milk gel at different observation levels, using bulk rheology and syringe compression test at the macroscopic level, passive particle tracking at the microscopic level and the PFG-NMR at the molecular level, upon acidification with GDL (2% w/w) with and without the presence of IC at low concentration (0.05% w/w).

2. Materials and methods

2.1. Materials

Skim milk powder (Yotsuba Milk Products Co., Ltd., Hokkaido, Japan), with a fat content of 0.7 g/100 g and protein content of 35.6 g/100 g, was used in all experiments. Acidulant GDL (>98.0%) and sodium-type ι-carrageenan powders were purchased from Tokyo Chemical Industry Co., Ltd. (Tokyo, Japan). IC was dialyzed against NaCl solution and subsequently against deionized water as described previously (Du, Brenner, Xie, & Matsukawa, 2016) to obtain Na + type carrageenan solutions. The concentration of Na+ and K+ of the dialyzed carrageenan were analyzed by inductively coupled plasma atomic emission (ICP) to be 0.63% and 0.105% respectively. No Mg + or Ca + ions were detected in the dialyzed sample (Geonzon, Bacabac, & Matsukawa, 2019b). For particle tracking, fluorescent-labeled polystyrene particles with different sizes (0.3 μm, Green and 1.0 μm, Red, Thermo Scientific Corp.) were used. For NMR measurements, poly(ethylene oxide) (PEO) with narrow M_w distribution (PEO SE-15: Mw 1.46 × 10^5; Mw/Mn 1.08, Tosoh Corp., Japan) were added to the sample as a probe polymer.

2.2. Preparation of reconstituted skim milk and acidification

Reconstituted skim milk was prepared by dispersing skim milk powder into distilled water to obtain a concentration of 11% (w/w). The total solid content of the milk was 8.50 ± 0.026% after 24 h at 105 °C. Reconstituted skim milk was heat-treated in a thermostatically controlled water bath at 85 °C for 30 min with a continuous stirring, and was immediately cooled in an ice bath to 30 °C. For another set of samples, dialyzed ι-carrageenan was added at a concentration of 0.05% of the milk sample (w/w) prior to the heat-treatment. For NMR, milk powder and 0.1% (w/w) PEO was dispersed in D_2O and heat-treated at 85 °C for 30 min. To all samples, GDL was added at the concentration of 2.0% (w/w) and thoroughly dissolved in the solution by mixing by hand for 1 min. The solution was incubated for 3 h at 30 °C.

2.3. pH and dynamic rheological measurements

The pH of the sample was measured at every 10–15 min during the incubation using a 640S-1 pH meter (Sato Keiryoki Mfg. Co. Ltd., Tokyo, Japan) until pH reached below 4.6. For dynamic rheological measurements, the sample was loaded into a HAAKE MARS II rheometer (Thermo Scientific, Waltham, MA, USA) equipped with a pre-heated coaxial cylinder at 30 °C (inner diameter 25 mm; outer diameter 27.5 mm) and time course measurements of storage and loss modulus (G′ and G″) were performed at 1 Hz frequency and 1% strain for up to 200 min. The experiments were done in triplicates. The obtained values were used to extrapolate values calculated using Mathematica 10 (Wolfram Research, Inc., Champaign, IL) and used to construct an average representation of the G′ and G″.

2.4. Syringe compression test

Immediately after mixing with 2.0% GDL (w/w), the sample was poured into an open end of a 5-mL plastic syringe (plunger diameter 13 mm; tip diameter 1.5 mm, Terumo, Tokyo, Japan), with the other end connected to a closed syringe with an L-shaped adapter (Supplementary Fig. 1). The compression test was performed at 0 (immediately after GDL addition), 15, 30, 60, 90, 120, 150 and 180 min of the incubation at 30 °C. At each time interval, the open end of the syringe was sealed with the plunger and placed in the stage connected to RCT-2002D-D Fudoh Rheometer (Rheotech, Tokyo, Japan) with a plastic support. The rheometer arm pushed the plunger of the syringe at the displacement rate of 6 cm/min, forcing the sample inside to flow through the other end of the syringe. This procedure was repeated from the other end, for three cycles resulting in total six measurements. The force (F_{total}) (N) exerted on the plunger of the syringe was continuously measured at every 0.02 s, and only the range corresponding to the duration of each compression was used to obtain the average of the F_{total} at each measurement. F_{total} was expressed as the sum of the frictional force F_{fri} (N) of the syringe, the force attributed to the sample viscosity F_{vis} (N), and the breaking force F_{bre} (N) of the sample as follow:

$$F_{total} = F_{fri} + F_{vis} + F_{bre}$$

F_{fri} was obtained using distilled water where F_{vis} was assumed to be negligible. The average F_{fri} was determined to be 0.956 N (±0.037) over the six measurements. F_{vis} was determined by subtracting F_{fri} from the

F_{total} obtained at the sixth measurement assuming no F_{bre}. F_{bre} was calculated by subtracting ($F_{fri} + F_{vis}$) obtained at the first measurement. The test was performed at room temperature in triplicates for each sample. Statistical analyses were performed on the average values using the SPSS statistics software package version 26 (SPSS Inc., Chicago, IL). General linear model (GLM) Univariate procedure in SPPS was used to examine the significant main effects of incubation time and IC addition on the F_{vis} and F_{bre}, followed by Tukey HSD post hoc test for the pair-wise comparison where appropriate. The significance level cut-off was set at 95% ($p < 0.05$).

2.5. Diffusion measurements by NMR

After adding 2.0 w/w % GDL, the sample with PEO at 30 °C was thoroughly mixed using vortex. The solution was immediately transferred into preheated (30 °C) 5 mm NMR tubes. The tubes containing the sample were then incubated at 30 °C. The diffusion coefficients (D) of PEO (D_{PEO}) in the sample were measured at 0, 15, 30, 45, 60, 90, 120, 150 and 180 min of incubation using a Bruker Advance 400WB spectrometer equipped with a diff60 probe and a pulse-gradient-stimulated-echo (PGSTE) pulse sequence (Stejskal & Tanner, 1965; Tanner, 1970). The D values were obtained by fitting the decay of the signal peak intensity with increased gradient strength using the following equation,

$$I(g) = I(0)\exp\left[-\gamma^2\delta^2 g^2 D\left(\Delta - \frac{\delta}{3}\right)\right]$$

where I(g) and I(0) are the echo signal intensities at $t = 2\tau 2 + \tau 1$ with and without field gradient, respectively, and γ is the gyromagnetic ratio of 1H. The gradient strength g was varied from 400 to 1000 G/cm with a gradient pulse length δ of 1 ms. The delay between the first and the second 90° pulses, τ2, and second and third 90° pulses, τ1, was set at 4.62 ms and 15.36 ms, respectively. The diffusion time Δ was set at 20 ms. The D of PEO (D_{PEO},0) in a dilute solution was measured using a sample of 0.1 w/w % PEO in D_2O at 30 °C, a temperature where convection is considered negligible (Zhao & Matsukawa, 2012).

2.6. Particle tracking

Particle tracking measurements of fluorescent-particles with different diameters (0.3 μm, Green and 1.0 μm, Red) were carried out using a BZ-9000 inverted microscope (Keyence Corp., Osaka, Japan) equipped with a PlanFluor 100 × NA 1.30 oil-immersion objective (Nikon Corp. Inc., Japan) and a temperature-controlled microscope stage (ALA Scientific Instruments Inc., New York). The fluorescent-labeled probe particles were added to the heat-treated and cooled sample at a concentration of 0.05% (w/w). Immediately after mixing with 2% GDL (w/w), the sample with the particles was transferred in a custom-made sample chamber (Geonzon, Bacabac, & Matsukawa, 2019a) equipped with a temperature sensor (CENTER 309, Center Technology Corp., Tokyo). The temperature of the sample chamber was maintained at 30 °C. The particle tracking was performed at 0, 15, 30, 45, 60, 90, 120 and 180 min of incubation. Videos of the diffusing fluorescent-labeled particles were recorded at a rate of 7.5 frames per second for 110 s using a built-in 2/3-inch, 1.5 megapixels, 12-bit, monochrome cooled CCD camera (Keyence Corp., Osaka, Japan). At the beginning of the incubation, the particles present in the sample without IC were observed to have high mobility. They occasionally moved in-and-out of focus during the tracking; thus, fewer particles (≈20–40 particles) were successfully tracked throughout the measurement.

Particle tracking and MSD calculations were performed using a custom-made program written in Mathematica 10 (Wolfram Research, Inc., Champaign, IL) described by Geonzon and Matsukawa (2019). Briefly, the position of each fluorescent-labeled particles was determined by an algorithm that improves the accuracy of particle position using the image-intensity weighted centroid for each particle, from which particle trajectories were formed and analyzed. The time-averaged MSD of each particle (msd) was obtained from N images representing a total diffusion time τ by the following equation (Lieleg, Vladescu, & Ribbeck, 2010; Wagner, Turner, Rubinstein, McKinley, & Ribbeck, 2017),

$$msd(\tau) = \frac{1}{N - \tau/\Delta t}\sum_{i=1}^{N-\frac{\tau}{\Delta t}} r\,(i\Delta t + \tau) - r\,(i\Delta t)^2$$

where Δt is the interval time for each frame expressed as the inverse of the frame rate, and $r(\Delta t)$ represents the position of the particle centroid. The exponent α in the relationship between msd and τ, $msd \sim \tau^{\alpha}$, was calculated for each particle in the range of τ from 1 to 10 s with a goodness of fit $R^2 \sim 0.99$. The particle tracking measurements were performed in duplicate to confirm the reproducibility of the measurements.

3. Results and discussion

3.1. pH and dynamic rheological measurements

Fig. 1a and b shows the average pH and representative graphs of storage modulus (G′) and loss modulus (G″) of the sample with and without IC during the incubation at 30 °C respectively. The initial pH of the sample was 6.56 ± 0.022 which decreased to ~4.5 within 180 min regardless of the IC addition. The sample without IC remained in the liquid state until it reached a sol-gel transition ($G' > G''$) at ~ pH 5.2 (~45 min) with the G′ and G″ values increasing rapidly afterwards. Prior to this transition, a drop in G′ and G″ was observed at a pH range ~5.3–5.2 (30 min), which may be attributed to the partial loosening of the weak initial gel network caused by the solubilization of colloidal calcium phosphate (CCP) (Lucey, 2017). With IC, the G′ of the sample was larger than the G″ at the start of incubation, indicating that the IC induced earlier milk gelation. Such early gelation has been attributed to micro-phase separation (depletion interactions), which reduces the molecular mobility of casein micelles promoting the casein-casein interactions and formation of loosely entangled aggregates at higher pH (Perrechil, Braga, & Cunha, 2009). Additionally, IC helices with their high charge density adsorb more readily onto the surface of the casein micelles (Wang et al., 2014) and can form a homogenous network at low concentrations (Arltoft, Ipsen, Madsen, & de Vries, 2007), thereby stabilizing the network structure through crosslinking of their molecular chains (Shchipunov & Chesnokov, 2003). The final G′ and G″ values of the samples were similar regardless of the IC addition, in agreement with several studies demonstrating that addition of polysaccharides at such low concentrations may not affect the final gel properties (Acero-Lopez et al., 2010; Kontogiorgos, Ritzoulis, Biliaderis, & Kasapis, 2006).

3.2. Syringe compression

The syringe compression test was aimed to quantify the force attributed to the sample viscosity (F_{vis}) as well as the breaking force of the gel (F_{bre}), as opposed to some texture deformation analysis on acid milk gel which are limited to the latter. Fig. 2a and b presents the average F_{bre} and F_{vis} of the sample with and without IC measured at 0, 15, 30, 45, 60, 90, 120, 150 and 180 min of the incubation at 30 °C, respectively. The F_{bre} of the sample was not significantly affected by the incubation time or the IC addition. On the other hand, the F_{vis} of the sample with and without IC increased steadily during the incubation and accounted for the strong main effect of the incubation time ($p < 0.001$), indicating that the changes in the total force (F_{total}) were largely dependent on the changes in the force attributed to the sample viscosity during the acid gelation. Regardless of IC addition, however, the F_{vis} of the sample did not significantly increase from its initial value until the later incubation stage (>120 min). Moreover, while the progressive

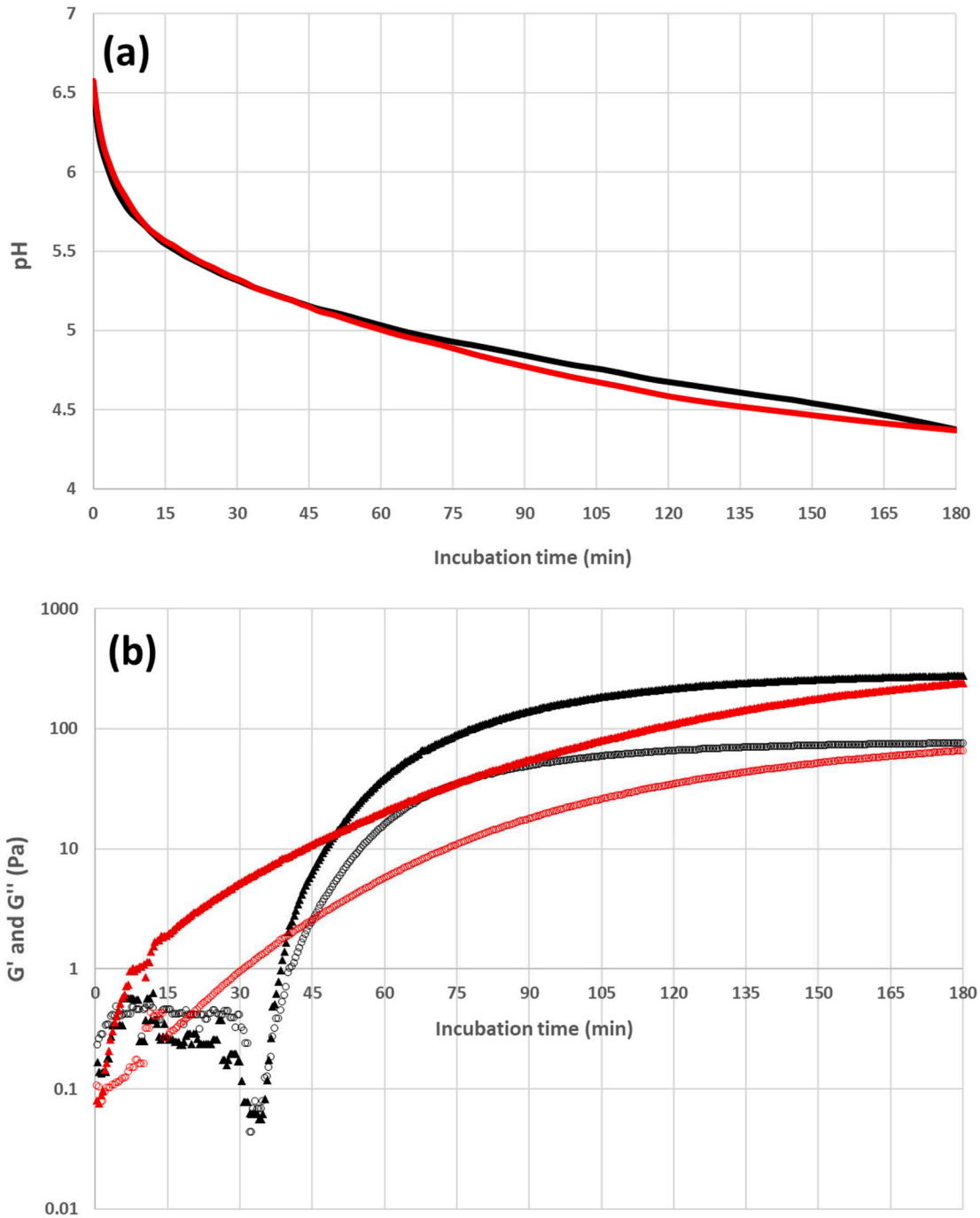

Fig. 1. a and b: The average pH (a) and a representative graph of filtered G′ (filled triangle) and G′′ (open circle) of the sample with (red) and without (black) IC (b).

increased in G′ and G′′ (where G′>G′′) indicated the early gelation in the IC sample (Fig. 1b), no significant difference in the F_{vis} was found between the sample with and without IC except at 30 min where the F_{vis} of the sample without IC was significantly lower than that of the IC sample ($p < 0.01$), corresponding to the drop in G′ and G′′ in the rheological measurement (Fig. 1b). The F_{vis} value was calculated at the sixth measurement after the sample had been pushed through the plunge multiple times, possibly disarranging some of the emerging/existing network structure of casein-casein, casein-carrageenan and/or carrageenan-carrageenan thus nullifying the effect on the sample viscosity, while at the later incubation (>120 min), the increased interaction and strengthening of the casein-casein aggregates and network structure may have accounted for the significant increase in F_{vis} in both samples. No significant difference was found in the final F_{vis} and F_{bre} of the sample with and without IC in agreement with the rheological observation at 180 min (Fig. 1b).

Fig. 3a and b shows the visual inspection of the sample with and without IC respectively, 1 h (at 30 °C) after the completion of the syringe compression test where the respective sample was pushed through the syringe six times at the time interval of 0, 15, 30, 45, 60, 90, 120, 150 and 180 min of incubation. At early incubation time up to 30 min, the sample without IC remained largely in liquid (Fig. 1b) which consequently formed a gel in the syringe at 30 °C (Fig. 3b). A clear phase separation of the serum and colloidal phase was seen in the sample at 45 and 60 min, before the proportion of the colloidal phase gradually increased later in the incubation (>90 min). The pH range at 45–60 min (~pH 5.1) is characterized by the extensive rearrangements of the internal structure of casein particles (Lucey, 2017). When compressed at

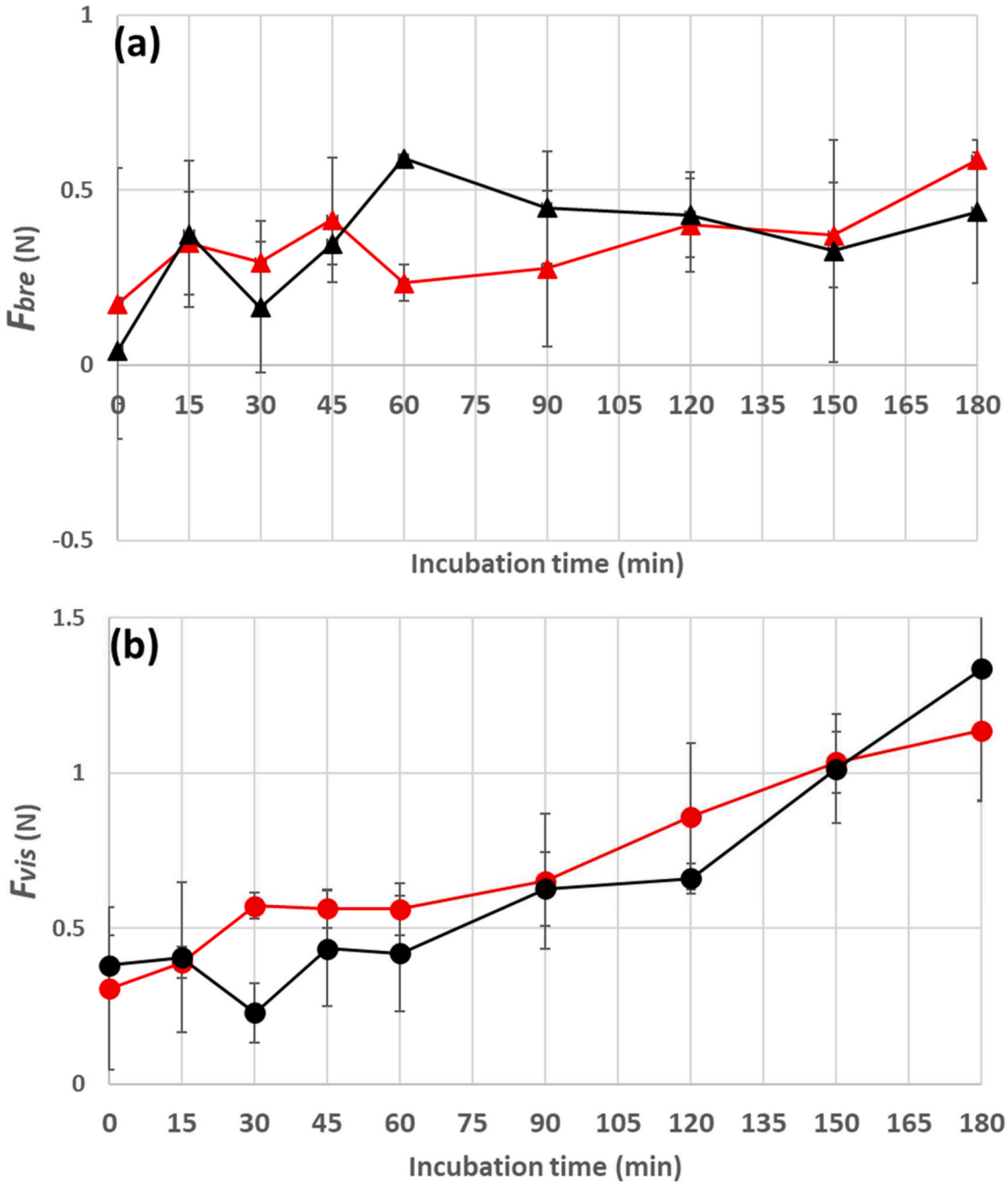

Fig. 2. a and b: The average breaking force F_{bre} (a) and force attributed to the viscosity F_{vis} (b) of the sample with (red) and without IC (black).

this critical stage, it seemed that the initial gel network of loosely entangled protein aggregates was destroyed in the sample, and subsequently the disrupted casein micelles reassociated into non-native colloidal structures which were unable to contain the serum phase. On contrary, when the pH was close to (pH $\leq$ 4.8, at >90 min) or below the isoelectric point of the casein, the existing network of chains and clusters formed in the sample seemed to contain the serum phase to a larger extent after the compression test. Non-covalent interactions, such as hydrophobic interactions increase at this pH range (Horne, 1998), which may have promoted the recovering capacity of the gel when subjected to large deformation (Nguyen, Wong, Guyomarc'h, Havea, & Anema, 2014).

With the presence of IC (Fig. 3a), the phase separation appeared already at the beginning of the incubation, indicating the emerging casein-carrageenan and/or carrageenan-carrageenan network structure. The degree of phase separation appeared to slightly increase at 15 min as the initial network continued to develop with time and destroyed after the compression, no longer able to hold the serum phase as seen in the sample without IC at 45–60 min. The extent of the phase separation decreased towards the later stage of the incubation, and the sample subjected to the compression at 150 and 180 min showed little phase separation following the test. Similarly, Ji et al. (2008) observed that casein/κ-carrageenan (0.025% 0.05% and 0.075%) aggregates in skim milk once formed were stable to shear (up to 1200 s^{-1}) which caused little change to their particle size distribution. As in the sample without IC, the role of hydrophobic interactions may explain the mitigated phase separation at later incubation stage.

3.3. Diffusion measurements by NMR

Fig. 4a shows representative PGSTE ^{1}H NMR spectra of milk sample with PEO (0.1% w/w). The peak at 3.7 ppm is assigned to PEO while the

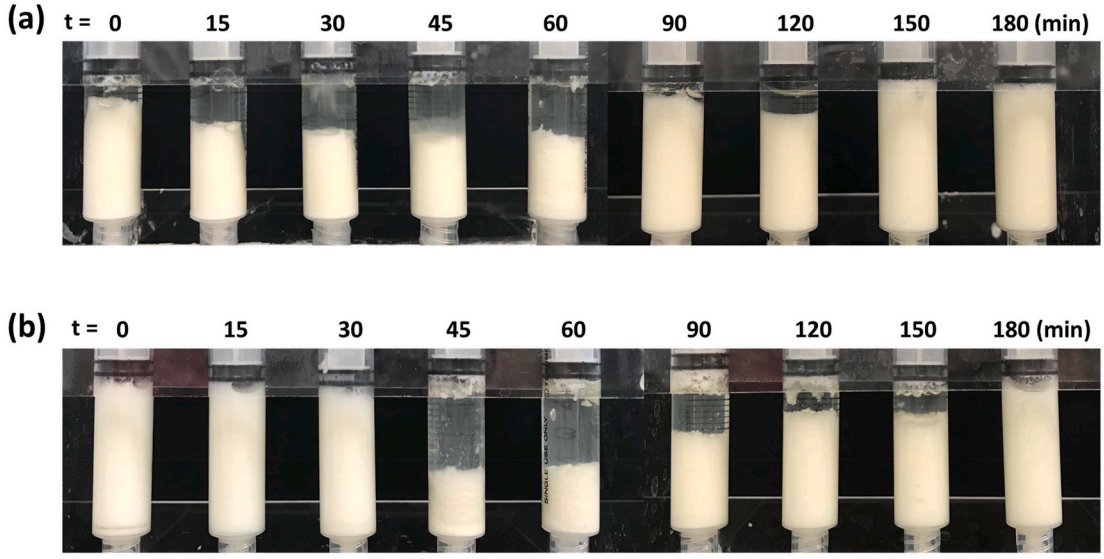

Fig. 3. a and b: Visual inspections of the sample with (a) and without IC (b) after 1 h at 30 °C following the after the completion of the syringe compression test where the respective sample was pushed through the syringe six times at the time interval 0, 15, 30, 45, 60, 90, 120, 150 and 180 min of incubation.

peak of water protons was not detected due to the large diffusivity of water at the applied *g*. The caseins have rigid sphere structures in the milk with acidulant, leading to the depression of casein peaks in the range from 0.3 to 2.5 ppm because of short ^{1}H T_2. On the other hand, the PEO peak remained showing the flexibility of PEO chain and the diffusion of PEO gives the information about the network changes of caseins (Matsukawa, Sagae, & Mogi, 2009). The semi-logarithmic plots of the signal decays of PEO in the milk gel with and without IC against $\gamma^2 g^2 \delta^2 (\Delta - \delta/3)$ gave straight lines (see the inset on Fig. 4b) indicating a unimodal diffusion process of PEO in the gel network.

Fig. 4b displays the change in the diffusion coefficients of PEO (D_{PEO}) for the samples with and without IC during the incubation. At the beginning of incubation, the behavior of the D_{PEO} corresponded to the rheological observation (Fig. 1b). In the presence of IC, the D_{PEO} of the sample increased progressively to the maximum at 30 min indicating early network formation, while the D_{PEO} without IC exhibited little change during the first 15 min before it rapidly increased to 30 min (pH ~5.3), in agreement with the onset of G′ and G″ increase from the rheological observation. At the critical pH range at ~30 min prior to the sol-gel transition, a collapse of the κ-casein hairy layer and casein particle dehydration reduce the mean diameter of casein micelles, while further enhancing electrostatic attraction between caseins (Alexander & Dalgleish, 2004; Lucey, 2017; McMahon et al., 2009). Although not observed by the rheological measurements without IC, the increased D_{PEO} at 30 min indicated that these extensive rearrangements occurred in both samples at the molecular level and decreased the volume occupied by obstructing elements for the probe, thus enlarging the diffusion space for PEO (Le Feunteun et al., 2008a).

Le Feunteun et al. (2008a) observed an increase in the probe diffusion coefficient during early acidification of concentrated casein systems using PEGs of similar molecular weight as in this study, even though the increase was observed at a higher pH (pH > 5.9). However, the development of the probe diffusion was not related to the sol-gel transition in the rheological measurement. A similar study by Le Feunteun, Ouethrani, and Mariette (2012) reported a decrease in the *D* of casein particles in correspondence with a decreasing phase angle ($\tan^{-1}$(G″/G′)) towards the sol-gel transition of a concentrated casein suspension, which was explained as a slowing down of the translational motions of the single particles by the emerging aggregates and clusters during the rennet coagulation. However, the effect of shortening of ^{1}HT_2 during the gelation was not discussed which is expected to affect the peak intensity. Several authors have reported an increase in the probe diffusion coefficient only after coagulation and during gel aging phase, reflecting the rearrangement of the gel structure and aggregate fusion leading to local matrix compaction and increased gel porosity and higher permeability (Colsenet et al., 2005; Le Feunteun & Mariette, 2008b; Salami et al., 2013).

On contrary, this study observed that D_{PEO} gradually decreased during 45–60 min (~pH 5.1) followed by a plateau (60–180 min) in both samples, whereas the macroscopic behavior was dependent of IC addition. As demonstrated by Matsukawa and Ando (1997), the decrease and plateau in the D_{PEO} after the sol-gel transition may be attributed to the loose complexation between the PEO and the network of the milk proteins, arising from the intermolecular hydrogen-bond interactions with the protein carboxyl groups under increasingly acidic conditions, restraining the segmental as well as translational motion of the probe. Similar decrease in the probe diffusion coefficient was observed during the gel aging phase of rennet-induced coagulation of a casein suspension, but only when using PEG of smaller molecular weight (620 g/mol) reflecting the reduction in the "through the casein aggregates" diffusion component (Le Feunteun et al., 2008b). In addition, the change of the diffusion coefficients of PEO and casein during and after coagulation are greatly influenced by probe molecular weight and flexibility (Salami et al., 2013), casein concentration (Colsenet et al., 2005), coagulation methods (Le Feunteun et al., 2008a) as well as incubation time and temperature affecting the acidification rate (Lee & Lucey, 2004), and these factors may also account for the reported variation in the diffusion behavior and its correspondence with the rheological observation.

3.4. Particle tracking

Fig. 5a shows the individual *msd* of 0.3 μm and 1.0 μm probe particles in the sample with and without IC up to 90 min of incubation at 30 °C. Particle tracking was performed up to 180 min, but no significant difference was observed in the particle distribution between 90 and 180 min. Fig. 5b presents the distributions of *msd*(5s) and α for the 0.3 μm particles in the sample with and without IC to further clarify the behavior of individual particles. In Fig. 5b, the micro-viscosity of the individual particles is represented by *msd*(5s), while the exponent α in the relationship MSD~τ^{α} is related to particle diffusion.

Without IC, the *msd* of both particles exhibited a diffusive behavior up to 30 min of the incubation (Fig. 5a) with α~1 (Fig. 5b), indicating a normal particle diffusion thus a purely viscous response of the surrounding medium. At 45 min, the 0.3 μm particles shifted towards lower

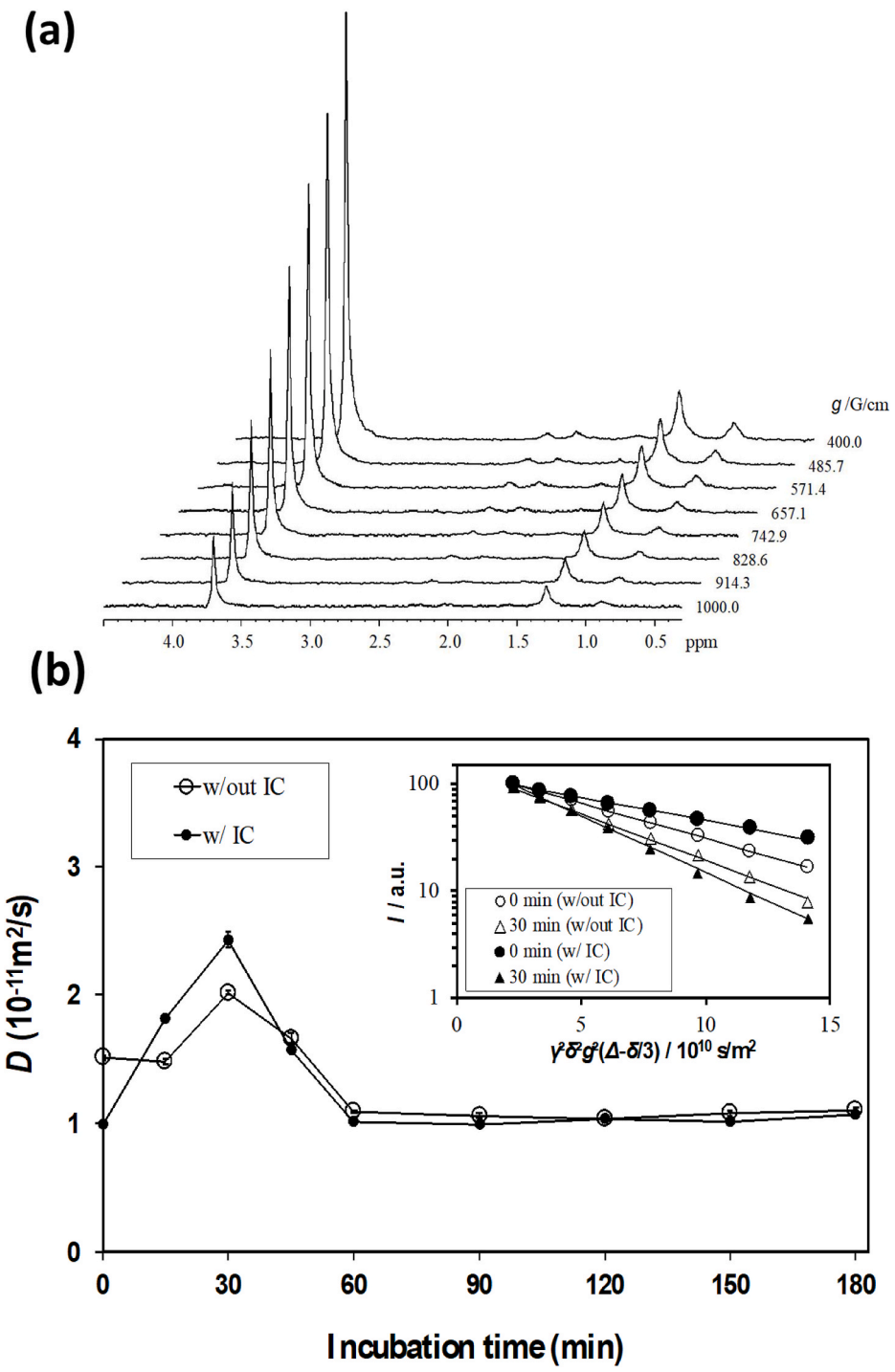

Fig. 4. a and b: Stacked attenuation spectra of diffusion measurements with PEO (a) and the diffusion coefficients of PEO in the sample with (open circle) and without (w/out) (closed circle) IC during the incubation (b). The inset figure shows the representative signal decays with the fitting (solid line) at 0 (circle) and 30 min (triangle) to obtain the diffusion coefficients using the equation, $I(g) = I(0)\exp\left[-\gamma^2\delta^2 g^2 D\left(\Delta - \frac{\delta}{3}\right)\right]$. Error bars represent the standard error in the fitting on the same equation.

α (Fig. 5b), and the lower and broader distribution of *msd* of 1.0 μm particles (Fig. 5a) signalized the development of increasingly restricted diffusion space in the medium, conferring some of the individual particles sub-diffusive (Gardel, Valentine, & Weitz, 2005; Mason & Weitz, 1995; Price, 2009) as the rapid increase in G′ and G″ took place in the macroscopic physical property of the sample (Fig. 1b). On the other hand, the *msd* of the 0.3 μm particles at 45 min without IC (Fig. 5a) indicated the formation of non-interconnected clusters (pores of network) of casein aggregates larger than the particle's diameter, allowing diffusion of these small particles (Waigh, 2005). With further incubation, the sample exhibited an abrupt decrease and ceased lag time-dependence of the *msd* of the 0.3 μm particles at 60 min followed by minimal motion at 90 min of both particles (Fig. 5a), indicating that the particle was increasingly arrested by the developing network, towards a more spatially uniform, interconnected elastic system (Cucheval et al., 2009; Moschakis et al., 2010).

With the presence of IC, the *msd* of the 0.3 μm probe particles exhibited sub-diffusive behavior with a broad distribution at the beginning of the incubation (Fig. 5a), suggesting the early formation of the heterogeneous network through the interaction/association between the IC and the milk proteins (Perrechil et al., 2009). This microscopic observation corresponded with the macroscopic measurements characterized by the progressive increase in G′ and G″ where G' > G″ during the early incubation (Fig. 1b). While promoting the gelation, the

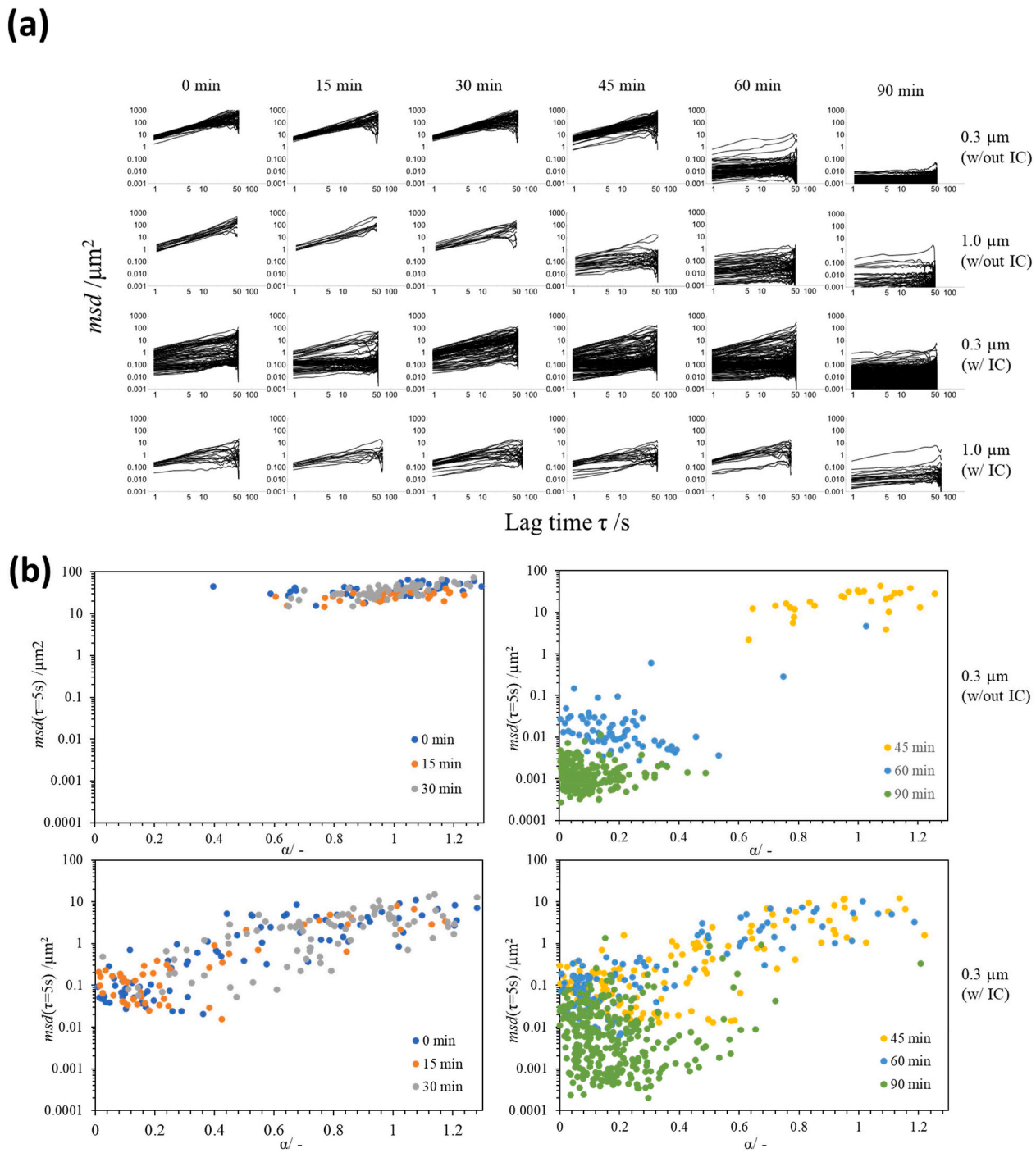

Fig. 5. a and b: Individual *msd* plot of 0.3 μm and 1.0 μm probe particles (a) and distribution of individual *msd* at τ = 5s plotted against exponent α for the 0.3 μm probe particles (b) for the sample with (w/) and without (w/out) IC at the different incubation time.

IC-induced local depletion surrounding the probe particles (depleted layers with increased porosity) (Sanchez, Zuniga-Lopez, Schmitt, Despond, & Hardy, 2000) may have caused local effects linked to the various length scales in the system, thus resulting in the large *msd* variation of the 0.3 μm probe particles. This corresponded with the wide scattering of the 0.3 μm probe particles at 0 and 15 min (Fig. 5b), followed by the shift towards higher *msd* and α at 30 min, suggesting an increase in the free space by the compaction of the developing network, in agreement with the NMR diffusion measurements (Fig. 4b). The sample without IC on the other hand did not show such shift at 30 min in the particle tracking, implying that IC altered the length scale of these network rearrangements occurring at the molecular level without IC to be detected at the microscopic level in the particle tracking of the IC sample. With further incubation, the distribution of *msd* and α of the particles again shifted downwards at 45–60 min (Fig. 5b), suggesting the growth of the aggregates with a high degree of heterogeneity. The further movement towards lower *msd* and α at 90 min reflected the increasing restrictions of particle mobility, whereas the broad distribution of the particles indicated a high degree of network heterogeneity still existing at this late incubation stage, in agreement with the continuous development of G′ and G″ in the macroscopic measurement (Fig. 1b). This contradicted with the drastic shift at 60–90 min observed in the sample without IC, indicating the rapid compaction of the formed network.

Moreover, at late incubation stage (45–60 min), the 1.0 μm particles with IC exhibited a narrower *msd* distribution than the 0.3 μm particles (Fig. 5a), indicating that the mobility of these larger particles were similarly restricted but more consistent within the IC-induced network structure. This contradicted with the sample without IC, which exhibited a wider *msd* distribution of the 1.0 μm particles at 45–60 min, indicating a varying degree of restricted particle movement. Moschakis et al. (2010) observed that probe particles, regardless of size (0.21, 0.32, 0.5, and 0.89 μm in diameter) and surface chemistry (polyethylene glycol, carboxylate groups and polystyrene), adsorbed onto the newly formed protein network at a pH close to the casein pI because of casein's strong adhesive properties and enhanced hydrophobic interactions at this pH range. Similar particle adsorption was detected at the void/protein network interface of acid milk gel by Cucheval et al. (2009) for uncoated and *k*-casein coated probe particles alike (0.46 μm in diameter, with increase of 10 nm when *k*-casein coated). The narrower *msd* distribution of the 1.0 μm particles with IC may reflect an increased particle adsorption through the IC-casein interaction, as demonstrated by Cucheval et al. (2009) with the addition of pectin (0.2%, w/w). On the other hand, it is possible that the movements of the smaller 0.3 μm particles were governed largely by the IC-induced local depletion in the system, introducing the wider *msd* distribution at 45 and 60 min. Without such IC-casein interaction, the 1.0 μm particles without IC may have been only partially adsorbed and/or incompletely covering the surface of the protein network because of their large size/surface area, binding capacity and/or adsorption characteristics (Valentine et al., 2004) e.g. steric hindrance, resulting in the modification of the local microstructure thus introduction of more heterogeneities than the 0.3 μm particles especially at 60 min. While Moschakis et al. (2010) observed no size-dependent behavior during GDL-induced gelation of sodium caseinate system (2–10% w/w sodium casein), analysis of individual mean square displacements, as opposed to the ensemble-averaged mean-squared displacement (Cucheval et al., 2009; Moschakis et al., 2010) may have allowed probing of the individual particle variation to a larger extent, thus revealing the size-dependent diffusion behavior in this study.

4. Conclusions

This work investigated the formation of acid milk gel at different length scales with and without the addition of *iota*-carrageenan (IC) (0.5% w/w) during incubation at 30 °C, using bulk rheology and syringe compression test at the macroscopic level, passive particle tracking with particles of diameters 0.3 and 1.0 μm at the microscopic level and PFG-NMR with PEO at the molecular level. Fig. 6 shows the schematic representation of the development of acid milk gel with and without addition of IC. The IC addition induced the early formation of the gel network in the sample as demonstrated by the progressive increase in G′ and G" (where G' > G″) in the macroscopic measurements. When repeatedly compressed during the developing stage, this formed network reassociated into non-native colloidal structures unable to contain the serum phase, which also occurred for the sample without IC but at later stage of incubation (>30 min) suggesting the importance of hydrophobic interactions. The increased PEO diffusion at 30 min in PFG-NMR reflected the emerging casein-casein network and its extensive rearrangement occurring at the molecular level in both samples. This corresponded only to the microscopic observation of the sample with IC, indicating that IC altered the length scale of the extensive network rearrangements and the subsequent enlargement of the diffusion space occurring at the molecular level to be detected at the microscopic level in the sample with IC. The size-dependency of the particle behaviors demonstrated a high degree of IC-induced network heterogeneity that continued to develop even at later incubation stage, on contrary to the drastic compaction of the formed network observed in the sample without IC.

CRediT authorship contribution statement

Izumi Sone: Conceptualization; Formal analysis; Validation; Visualization; Funding acquisition; Investigation; Methodology; Project administration; Resources; Writing-original draft; Writing-review & editing. Moe Hosoi: Investigation; Validation; Writing-original draft. Lester C. Geonzon: Conceptualization; Data curation; Formal analysis; Methodology; Software; Validation; Visualization; Writing-original draft. Hwabin Jung: Investigation; Validation; Data curation; Formal analysis; Visualization; Writing-original draft; Writing-review & editing.

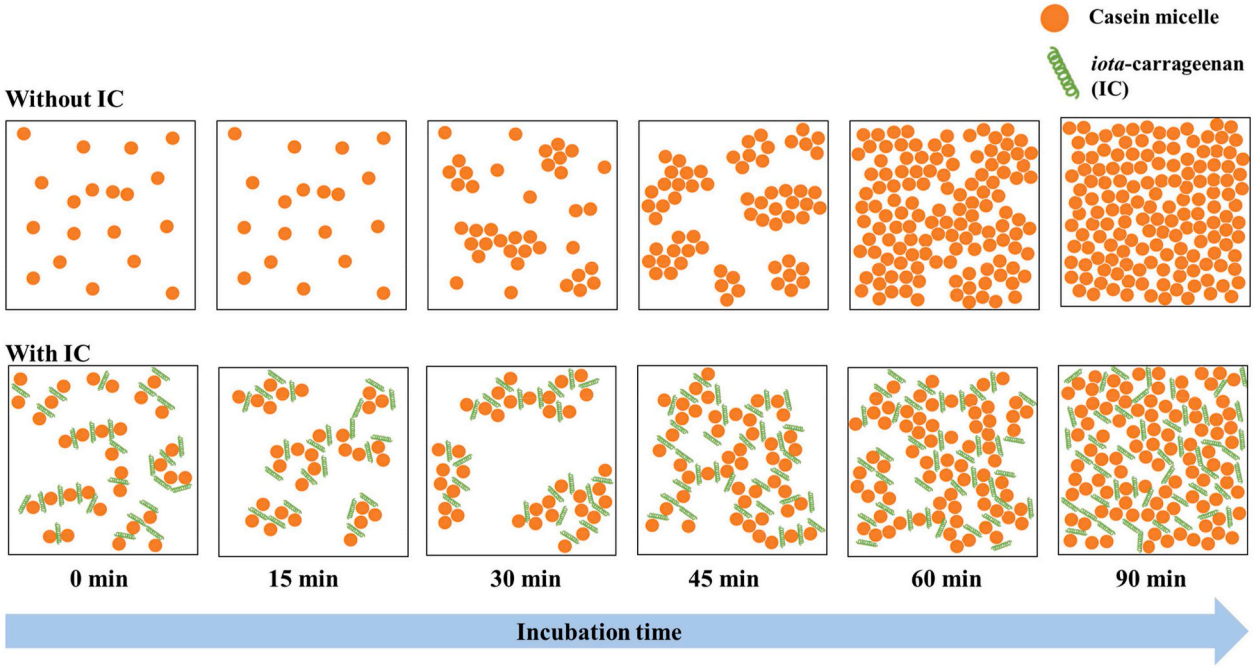

Fig. 6. Schematic representation of the formation of acid milk gel with and without addition of IC during incubation at 30 °C.

Faith Bernadette Descallar: Investigation; Validation; Data curation; Formal analysis; Visualization; Writing-original draft. Hu Bingjie: Visualization; Writing-original draft. Shingo Matsukawa: Supervision; Conceptualization; Methodology; Software; Resources; Funding acquisition; Project administration; Writing-original draft; Writing-review & editing.

Declaration of competing interest

The authors declare no conflict of interest.

Acknowledgement

This work was supported by the Research Council of Norway and the Norwegian Agency for International Cooperation and Quality Enhancement in Higher Education [grant number 309590]; the Research Council of Norway [grant numbers 281106and 194050]; The Scandinavia-Japan Sasakawa Foundation [GA19-NOR-0071]; JSPS KAKENHI [grant numbers JP18H00962and 20F20388].

Appendix A. Supplementary data

Supplementary data to this article can be found online at https://doi.org/10.1016/j.foodhyd.2021.107170.

References

Acero-Lopez, A., Alexander, M., & Corredig, M. (2010). Diffusing wave spectroscopy and rheological studies of rennet-induced gelation of skim milk in the presence of pectin and κ-carrageenan. *International Dairy Journal, 20*(5), 328–335.

Alexander, M., & Dalgleish, D. G. (2004). Application of transmission diffusing wave spectroscopy to the study of gelation of milk by acidification and rennet. *Colloids and Surfaces B: Biointerfaces, 38*(1), 83–90.

Arltoft, D., Ipsen, R., Madsen, F., & de Vries, J. (2007). Interactions between carrageenans and milk proteins: A microstructural and rheological study. *Biomacromolecules, 8*(2), 729–736.

Balakrishnan, G., Durand, D., & Nicolai, T. (2011). Particle diffusion in globular protein gels in relation to the gel structure. *Biomacromolecules, 12*(2), 450–456.

Caggioni, M., Spicer, P. T., Blair, D. L., Lindberg, S. E., & Weitz, D. A. (2007). Rheology and microrheology of a microstructured fluid: The gellan gum case. *Journal of Rheology, 51*(5), 851–865.

Cavallieri, A. L. F., Fialho, N. A. V., & Cunha, R. L. (2011). Sodium caseinate and κ-carrageenan interactions in acid gels: Effect of polysaccharide dissolution temperature and sucrose addition. *International Journal of Food Properties, 14*(2), 251–263.

Colsenet, R., Soderman, O., & Mariette, F. (2005). Effect of casein concentration in suspensions and gels on poly(ethylene glycol)s NMR self-diffusion measurements. *Macromolecules, 38*(22), 9171–9179.

Corredig, M., Sharafbafi, N., & Kristo, E. (2011). Polysaccharide–protein interactions in dairy matrices, control and design of structures. *Food Hydrocolloids, 25*(8), 1833–1841.

Cucheval, A. S. B., Vincent, R. R., Hemar, Y., Otter, D., & Williams, M. A. K. (2009). Multiple particle tracking investigations of acid milk gels using tracer particles with designed surface chemistries and comparison with diffusing wave spectroscopy studies. *Langmuir, 25*(19), 11827–11834.

Drohan, D. D., Tziboula, A., McNulty, D., & Horne, D. S. (1997). Milk protein-carrageenan interactions. *Food Hydrocolloids, 11*(1), 101–107.

Du, L., Brenner, T., Xie, J., & Matsukawa, S. (2016). A study on phase separation behavior in kappa/iota carrageenan mixtures by micro DSC, rheological measurements and simulating water and cations migration between phases. *Food Hydrocolloids, 55*, 81–88.

Gardel, M. L., Valentine, M. T., & Weitz, D. A. (2005). Microrheology. In K. S. Breuer (Ed.), *Microscale diagnostic techniques* (pp. 1–49). Springer.

Geonzon, L. C., Bacabac, R. G., & Matsukawa, S. (2019a). Microscopic characterization of phase separation in mixed carrageenan gels using particle tracking. *Journal of the Electrochemical Society, 166*(9), B3228–B3234.

Geonzon, L. C., Bacabac, R. G., & Matsukawa, S. (2019b). Network structure and gelation mechanism of kappa and iota carrageenan elucidated by multiple particle tracking. *Food Hydrocolloids, 92*, 173–180.

Geonzon, L. C., & Matsukawa, S. (2019). Accuracy improvement of centroid coordinates and particle identification in particle tracking technique. *Journal of Biorheology, 33*(1), 2–7.

Horne, D. S. (1998). Casein interactions: Casting light on the black boxes, the structure in dairy products. *International Dairy Journal, 8*(3), 171–177.

Hu, B., Lu, Y., Zhao, Q., & Matsukawa, S. (2017). A study on the gelation behavior of solutions of native gellan, deacylated gellan, and their mixture by water 1H T2 measurements. *Food Hydrocolloids, 72*, 47–51.

Ji, S., Corredig, M., & Goff, H. D. (2008). Aggregation of casein micelles and κ-carrageenan in reconstituted skim milk. *Food Hydrocolloids, 22*(1), 56–64.

Kontogiorgos, V., Ritzoulis, C., Biliaderis, C. G., & Kasapis, S. (2006). Effect of barley β-glucan concentration on the microstructural and mechanical behaviour of acid-set sodium caseinate gels. *Food Hydrocolloids, 20*(5), 749–756.

Langendorff, V., Cuvelier, G., Launay, B., Michon, C., Parker, A., & De Kruif, C. G. (1999). Casein micelle/iota carrageenan interactions in milk: Influence of temperature. *Food Hydrocolloids, 13*(3), 211–218.

Langendorff, V., Cuvelier, G., Michon, C., Launay, B., Parker, A., & De kruif, C. G. (2000). Effects of carrageenan type on the behaviour of carrageenan/milk mixtures. *Food Hydrocolloids, 14*(4), 273–280.

Le Feunteun, S., & Mariette, F. (2008a). Effects of acidification with and without rennet on a concentrated casein system: a kinetic NMR probe diffusion study. *Macromolecules, 41*(6), 2079–2086.

Le Feunteun, S., & Mariette, F. (2008b). PFG−NMR techniques provide a new tool for continuous investigation of the evolution of the casein gel microstructure after renneting. *Macromolecules, 41*(6), 2071–2078.

Le Feunteun, S., Ouethrani, M., & Mariette, F. (2012). The rennet coagulation mechanisms of a concentrated casein suspension as observed by PFG-NMR diffusion measurements. *Food Hydrocolloids, 27*(2), 456–463.

Lee, W. J., & Lucey, J. A. (2004). Structure and physical properties of yogurt gels: Effect of inoculation rate and incubation temperature. *Journal of Dairy Science, 87*(10), 3153–3164.

Lieleg, O., Vladescu, I., & Ribbeck, K. (2010). Characterization of particle translocation through mucin hydrogels. *Biophysical Journal, 98*(9), 1782–1789.

Lucey, J. A. (2016). Acid coagulation of milk. In P. L. H. McSweeney, & J. A. O'Mahony (Eds.), *Advanced dairy chemistry: Volume 1B: Proteins: Applied aspects* (pp. 309–328). Springer.

Lucey, J. A. (2017). Formation, structural properties, and rheology of acid-coagulated milk gels. In P. L. H. McSweeney, P. F. Fox, P. D. Cotter, & D. W. Everett (Eds.), *Cheese* (pp. 179–197). Academic Press.

Lucey, J. A., Tamehana, M., Singh, H., & Munro, P. A. (1998). A comparison of the formation, rheological properties and microstructure of acid skim milk gels made with a bacterial culture or glucono-δ-lactone. *Food Research International, 31*(2), 147–155.

Martin, A. H., Douglas Goff, H., Smith, A., & Dalgleish, D. G. (2006). Immobilization of casein micelles for probing their structure and interactions with polysaccharides using scanning electron microscopy (SEM). *Food Hydrocolloids, 20*(6), 817–824.

Mason, T. G., & Weitz, D. A. (1995). Optical measurements of frequency-dependent linear viscoelastic moduli of complex fluids. *Physical Review Letters, 74*(7), 1250–1253.

Matsukawa, S., & Ando, I. (1997). Study of self-diffusion of molecules in a polymer gel by pulsed-gradient spin-echo 1H NMR. 2. Intermolecular hydrogen-bond interaction between the probe polymer and network polymer in N,N-dimethylacrylamide−acrylic acid copolymer gel systems. *Macromolecules, 30*(26), 8310–8313.

Matsukawa, S., Sagae, D., & Mogi, A. (2009). Molecular diffusion in polysaccharide gel systems as observed by NMR. In M. Tokita, & K. Nishinari (Eds.), *Gels: Structures, properties, and functions. Progress in colloid and polymer science* (pp. 171–176). Springer.

McMahon, D. J., Du, H., McManus, W. R., & Larsen, K. M. (2009). Microstructural changes in casein supramolecules during acidification of skim milk. *Journal of Dairy Science, 92*(12), 5854–5867.

Moschakis, T. (2013). Microrheology and particle tracking in food gels and emulsions. *Current Opinion in Colloid & Interface Science, 18*(4), 311–323.

Moschakis, T., Murray, B. S., & Dickinson, E. (2010). On the kinetics of acid sodium caseinate gelation using particle tracking to probe the microrheology. *Journal of Colloid and Interface Science, 345*(2), 278–285.

Nguyen, N. H. A., Wong, M., Guyomarc'h, F., Havea, P., & Anema, S. G. (2014). Effects of non-covalent interactions between the milk proteins on the rheological properties of acid gels. *International Dairy Journal, 37*(2), 57–63.

Pang, Z., Deeth, H., Sharma, R., & Bansal, N. (2015). Effect of addition of gelatin on the rheological and microstructural properties of acid milk protein gels. *Food Hydrocolloids, 43*, 340–351.

Perrechil, F. A., Braga, A. L. M., & Cunha, R. L. (2009). Interactions between sodium caseinate and LBG in acidified systems: Rheology and phase behavior. *Food Hydrocolloids, 23*(8), 2085–2093.

Price, W. S. (2009). *NMR studies of translational motion: Principles and applications*. Cambridge: Cambridge University Press.

Salami, S., Rondeau-Mouro, C., van Duynhoven, J., & Mariette, F. (2013). Probe mobility in native phosphocaseinate suspensions and in a concentrated rennet gel: Effects of probe flexibility and size. *Journal of Agricultural and Food Chemistry, 61*(24), 5870–5879.

Sanchez, C., Zuniga-Lopez, R., Schmitt, C., Despond, S., & Hardy, J. (2000). Microstructure of acid–induced skim milk–locust bean gum–xanthan gels. *International Dairy Journal, 10*(3), 199–212.

Shchipunov, Y. A., & Chesnokov, A. V. (2003). Carrageenan gels in skim milk: formation and rheological properties. *Colloid Journal, 65*(1), 105–113.

Spagnuolo, P. A., Dalgleish, D. G., Goff, H. D., & Morris, E. R. (2005). Kappa-carrageenan interactions in systems containing casein micelles and polysaccharide stabilizers. *Food Hydrocolloids, 19*(3), 371–377.

Stejskal, E. O., & Tanner, J. E. (1965). Spin diffusion measurements: Spin echoes in the presence of a time-dependent field gradient. *The Journal of Chemical Physics, 42*(1), 288–292.

Tanner, J. E. (1970). Use of the stimulated echo in nmr diffusion studies. *The Journal of Chemical Physics, 52*(5), 2523–2526.

Valentine, M. T., Perlman, Z. E., Gardel, M. L., Shin, J. H., Matsudaira, P., Mitchison, T. J., et al. (2004). Colloid surface chemistry critically affects multiple particle tracking measurements of biomaterials. *Biophysical Journal, 86*(6), 4004–4014.

Wagner, C. E., Turner, B. S., Rubinstein, M., McKinley, G. H., & Ribbeck, K. (2017). A rheological study of the association and dynamics of MUC5AC gels. *Biomacromolecules, 18*(11), 3654–3664.

Waigh, T. A. (2005). Microrheology of complex fluids. *Reports on Progress in Physics, 68*(3), 685–742.

Wang, F., Liu, X., Hu, Y., Luo, J., Lv, X., Guo, H., et al. (2014). Effect of carrageenan on the formation of rennet-induced casein micelle gels. *Food Hydrocolloids, 36*, 212–219.

Zhao, Q., & Matsukawa, S. (2012). Estimation of the hydrodynamic screening length in κ-carrageenan solutions using NMR diffusion measurements. *Polymer Journal, 44*(8), 901–906.